Chapter 3

Reaction Growth of MF_2/*a*-C (M = Ca, Mg) Core/Shell Nanowires at the Interface of Vapor and Solid Reactants

3.1 Introduction

Fluorides of calcium and magnesium, CaF_2 and MgF_2 are high melting, low aqueous solubility, and very large band-gap ionic crystals.[1-3] They have been applied widely in chemical, metallurgical and optical industries. Recently, their potential applications in other technology areas such as devices and catalysis have been explored.[4-9] Due to their low volatility, lack of simple precursors, and low solubility in common solvents, controlled growth of these fluorides into various nanosized shapes has been a complex challenge.[10-12] Methods to direct their growth into one-dimensional nanostructures are unknown. This contrasts to the widely available processes for growing metal and semiconductor nanowires in large quantities, such as vapor transport, vapor-liquid-solid (VLS), chemical vapor deposition (CVD), and micelle assisted solution methods.[13,14] Here, we report the first high yield synthesis of CaF_2/*a*-C and MgF_2/*a*-C core/shell nanowires via simple vapor-solid reaction growth (VSRG).[15,16]

3.2 Experimental Section

3.2.1 Synthesis of MF_2/a-C (M = Ca, Mg) core/shell nanowires

Typically, C_6F_6 (99 %, Aldrich) was evaporated under bubbling Ar (5 sccm) at 273 K 1 atm into a tubular reactor loaded with CaC_2 (80 %, Aldrich) in an aluminum oxide boat. The reaction, carried out at a temperature 923 - 1273 K for 12 h, offered a black powder product **A** after workup. To prepare analogous products containing Mg, the following

reaction steps were also explored. Mg_3N_2 (99.5%, Aldrich) was pyrolyzed first at 1138 K under Ar (1 atm) for 1 h. Then, C_6F_6 was introduced by bubbling under a constant flow of Ar (5sccm) into the reactor maintained at 1138 K for 18 h. This generated a black powder **B**.

3.2.2 Characterization of MF_2/a-C (M = Ca, Mg) core/shell nanowires

Scanning electron microscope (SEM, JEOL JSM-6330F at 15 kV and HITACHI S-4000 at 25 kV), transmission electron microscopy (TEM, Philips TECNAI 20, operated at 200 kV) and high-resolution transmission electron microscope (HRTEM, JEOL JEM-4000 at 400 kV) were used to observe the sample morphology. Energy dispersive X-ray spectroscopy (EDS) was used to confirm the element composition of the samples. Crystallinity of the samples was investigated by an X-ray diffractometer (XRD, BRUKER AXS D8 ADVANCE, Cu K_α radiation, 40 kV and 40 mA).

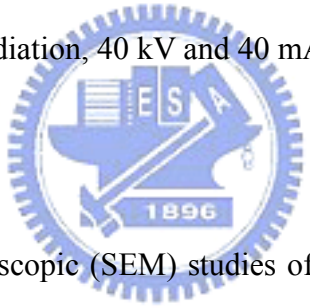

3.3 Results

Scanning electron microscopic (SEM) studies of the samples **A** and **B** are shown in Figure 3.1. A low magnification SEM image in Figure 3.1A, shows that a sample **A** synthesized at 973 K for 12 h is relatively straight wires several tens of micrometers in length. A high-magnification SEM image (Figure 3.1B) reveals that the 1-D solid is tens of nanometers in diameter. Using energy-dispersive spectroscopy (EDS), the elements in **A** are identified to be composed of C, F, and Ca (Figure 3.1C). Increasing the reaction temperature increased the diameter and the C concentration of the 1-D product. The product formed at 1273 K was essentially carbon rods of several micrometers in diameter. From Figure 3.1, panels D and E, the SEM images of **B** grown at 1138 K for 18 h, the wire length and diameter are estimated to be tens of micrometers and 60 - 100 nm, respectively. The EDS in Figure 3.1F confirms that the sample consists of C, F, and Mg.

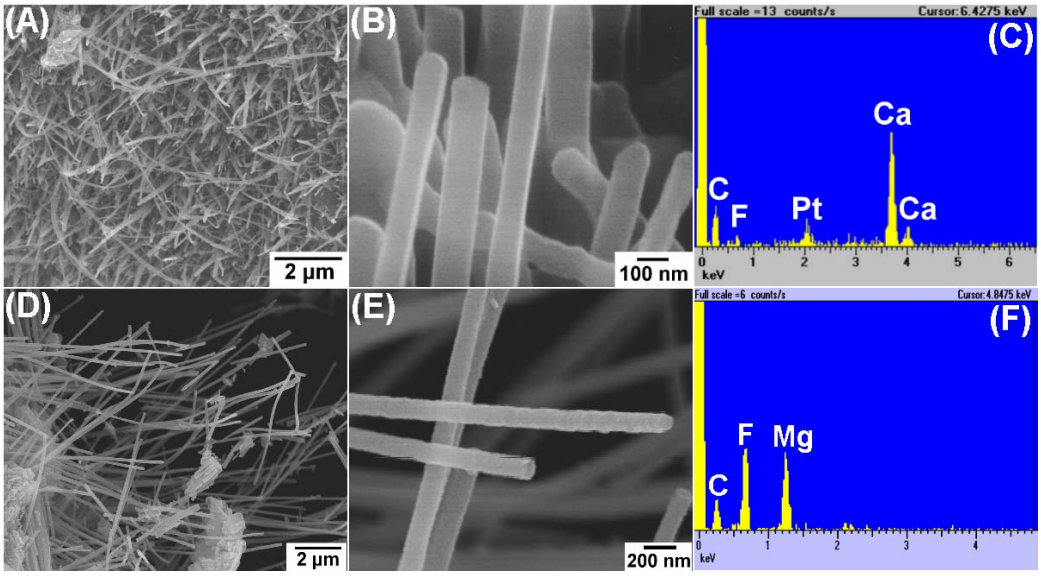

Figure 3.1 (A) SEM (low magnification), (B) SEM (high magnification) and (C) EDS of CaF_2/*a*-C nanowires prepared at 973 K; (D) SEM (low magnification), (E) SEM (high magnification) and (F) EDS of MgF_2/*a*-C nanowires prepared at 1138 K.

X-ray diffraction study of **A** synthesized at 973 K showed that the reflections can be indexed to a cubic fluorite structure with a lattice constant *a* of ca. 0.546 nm. This is comparable to the literature value of CaF_2, *a* = 0.5463 nm (JCPDS 35-0816). On the basis of the XRD and the EDS data, we conclude that the reactant CaC_2 was quantitatively converted to CaF_2, a mjor component in **A**, above 923 K. After a reaction at 923 K for 12 h, the XRD patterns of CaF_2 and CaC_2 still coexisted. Below this temperature, there was little sign of CaF_2 formation (Figure 3.2). Although carbon was detected as a main constituent in **A** by EDS, there were no reflection signals assignable to any type of crystalline carbon phases. Thus, the carbon elements probably coexisted with the CaF_2 crystals in an amorphous state. Data from the XRD and EDS studies also suggested that **B**, produced at 1138 K, contained pure tetragonal phase MgF_2 with esimated lattice constants *a* = 0.462 nm and *c* = 0.305 nm (JCPDS 41-1443) and some amorphous carbon material.

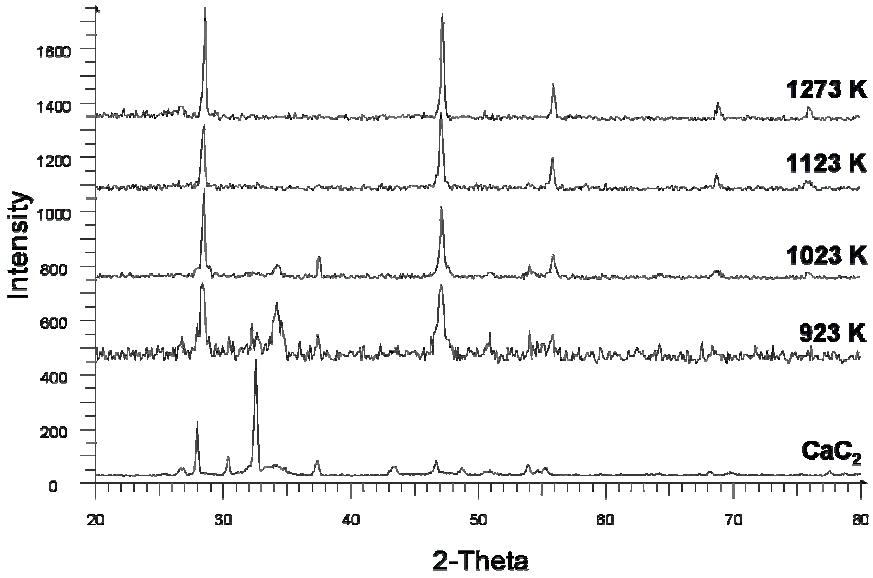

Figure 3.2 XRD patterns of the reactant CaC_2 and the product CaF_2 grown at temperatures 923 – 1273 K for 4 h.

The samples were further investigated by transmission electron microscopy and the images are shown in Figure 3.3. A low-magnification image in Figure 3.3A shows a straight wire of **A** with a diameter of ca. 60 nm. A dot pattern (inset of Figure 3.3A) from the selected area electron diffraction (SAED) suggests that the sample is single crystalline. From the pattern, the observation is indexed to the [1 -1 -2] zone axis of a fluorite structure. The lattice parameter *a* is estimated to be 0.542 nm, close to the *a* value of CaF_2, 0.5463 nm (JCPDS 35-0816). A representative high-resolution TEM (HRTEM) image of **A** is shown in Figure 3.3B. A boxed area in Figure 3.3B, enlarged in the inset, shows that the lattice fringes are spaced 0.313 nm apart. The distance coincides well with the {111} interplanar distance of CaF_2. Combined with the SAED result, the nanowire growth is determined to be along the [1 1 0] direction of CaF_2. In Figure 3.2B, in addition to the crystalline core of CaF_2, a shell of amorphous material of ca. 15 nm is also observed. Based on the EDS result, the amorphous material is identified to be carbon. TEM images shown in Figure 3.3C reveal that an individual nanowire **B** grown at 1138 K has a diameter of ca. 70 nm.

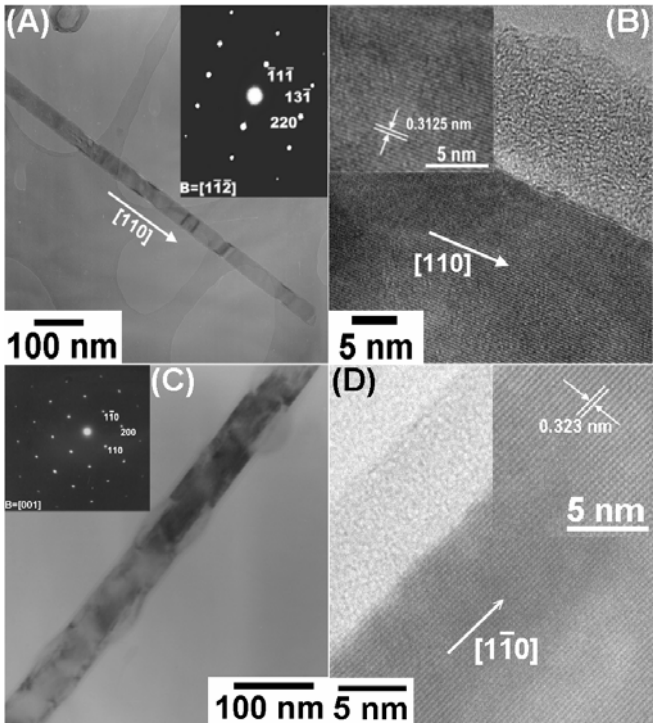

Figure 3.3 (A) TEM (low magnification) and SAED (inset), and (B) HRTEM and enlarged view (inset) of a CaF_2/*a*-C nanowire prepared at 973 K; (C) TEM (low magnification) and SAED (inset), and (D) HRTEM and enlarged view (inset) of a MgF_2/*a*-C nanowire prepared at 1138 K.

The SAED (inset in Figure 3.3C) pattern is indexed to the [0 0 1] zone axis of the tetragonal phase MgF_2. From the HRTEM images in Figure 3.3D, spacing of the observed fringes is estimated to be 0.323 nm, which corresponds to the {110} interplanar distance of tetragonal MgF_2. The nanowire growth direction is determined to be along the [1 -1 0] axis of MgF_2. In addition, from the image and the EDS result, the presence of an amorphous carbon shell of ca. 7 nm is identified outside the MgF_2 core.

3.4 Discussion

On the basis of the experimental data presented above, we conclude that the samples **A** and **B** are CaF_2/*a*-C and MgF_2/*a*-C core/shell nanowires, respectively. Growth of the CaF_2/*a*-C nanowires is further discussed below to illustrate the important features of the reaction. The overall stoichiometry between C_6F_6 and CaC_2 to produce CaF_2 and C is proposed to be $C_6F_6 + 3\ CaC_2 \rightarrow 3\ CaF_2 + 12\ C$. This is a thermodynamically favored reaction with an estimated standard Gibbs free energy of reaction (ΔG_r^o) of -2447.6 kJ/mol

per mole of C_6F_6 consumed.[18] The reaction is highly exothermic because of the high standard Gibbs free energy of formation (ΔG_f^o) of CaF_2, -1173.5 kJ/mol.[18] Even though the reaction is highly exothermic, the observed CaF_2/*a*-C nanowire growth rate was extremely slow below 923 K. The strong C-F bonds in C_6F_6 probably generated high energy reaction barriers.[1] Literature data indicated that the decomposition of C_6F_6 starts at about 923 K.[17] Above the temperature threshold, highly reactive and short living intermediates, such as CF, CF_2, and CF_3, are produced and should react favorably with the CaC_2 surface to generate the products. At high temperatures, the C_xF_y species may react in another pathway, to disproportionate into materials with thick carbon layers and saturated fluorocarbon molecules. To rationalize how the products CaF_2 and *a*-C grow into a 1D core/shell nanostructure, a simple VSRG mechanism is proposed in Scheme 3.1. The reaction happens at the vapor-solid interface near the surface of CaC_2. With proper seeding, this surface can provide an environment that enhances the growth of solid products in certain dimensions. Both of the products, crystalline CaF_2 and amorphous carbon, are low volatile and high melting solids, 1676 and 3823 K (graphite), respectively. Due to their large difference in surface energies, the as-formed nanoparticles probably were composed of a phase-separated CaF_2 core covered with an *a*-C shell. These nanoparticles may act as seeds, migrate and coalesce, then grow into nanowires.

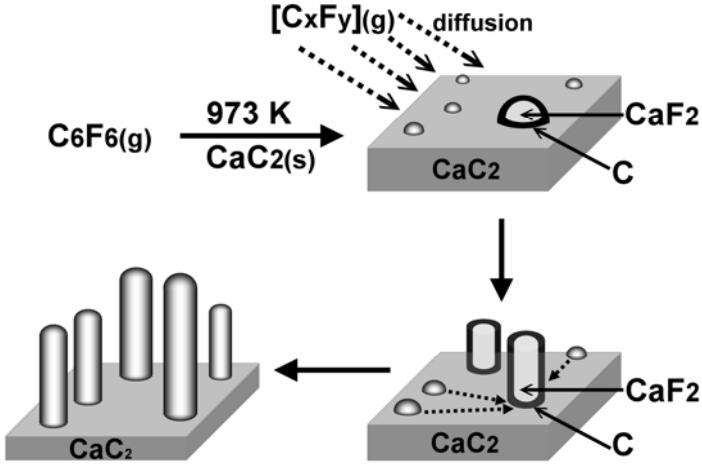

Scheme 3.1 Proposed Pathway to Form CaF_2/*a*-C Nanowires.

An HRTEM study (Figure 3.4) of a nanowire **A**, grown at 973 K for 12 h, displayed a diameter of ca. 30 nm and a round-shaped top-end. This suggests that at this stage, the carbon shell was yet to be thickened. The nanowire probably elongated through a bottom-up growth mechanism instead of a tip growth mechanism. Thus, we suggest in Scheme 3.1 that the as-produced CaF_2/*a*-C nanoparticles on the CaC_2 surface migrates and incorporates into the root portion of the nanowires. From here, CaF_2 and *a*-C extend cooperatively as interdependent self-templates. Since the growth temperature employed, 973 K, was far below the melting points of CaF_2 and *a*-C, nanowires with limited diameters were obtained. At high growth temperature or prolonged reaction time, the reactant CaC_2 can be totally consumed. Under this condition, significant thickening of the carbon layer, probably enhanced by gas phase decomposition of C_6F_6 mentioned above, widened the wire diameter (Figure 3.5). The arguments presented above can rationalize the growth of nanowires **B** also.

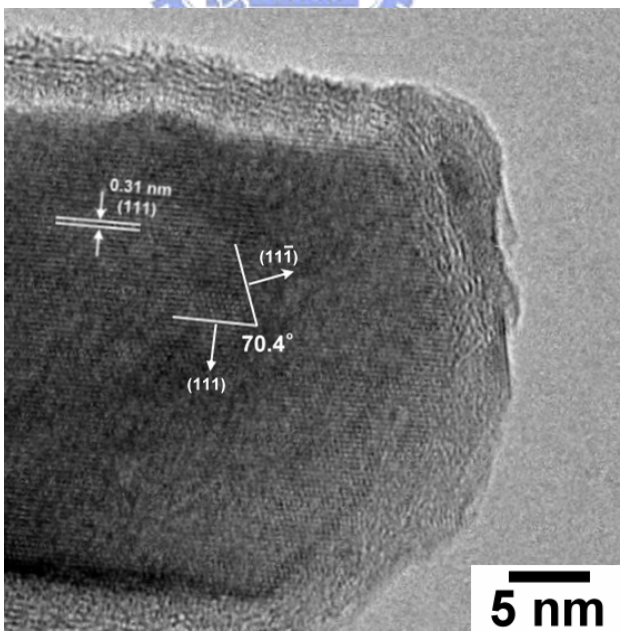

Figure 3.4 HRTEM image of the end of a CaF_2/*a*-C nanowire grown at 973 K for 12 h.

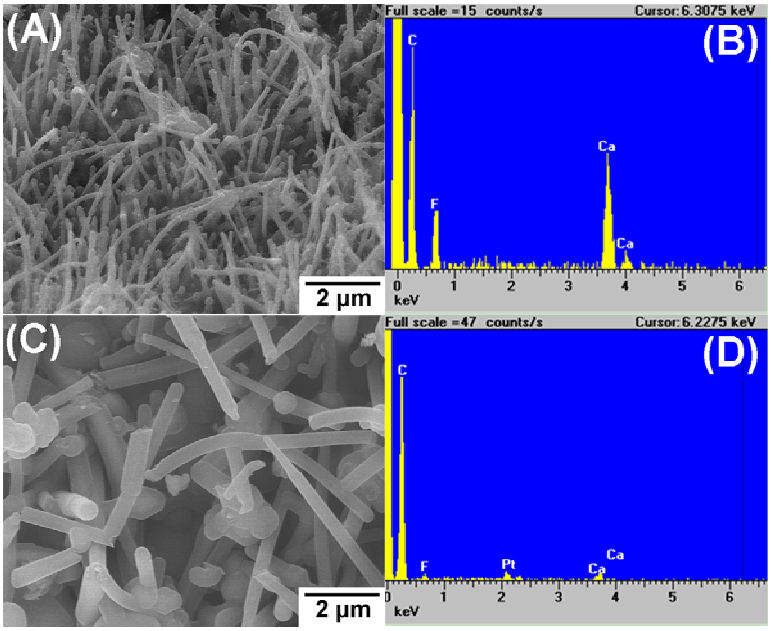

Figure 3.5 CaF_2/*a*-C nanowires grown at various temperatures for 4 h. 1023 K: (A) SEM and (B) EDS, 1273 K: (C) SEM and (D) EDS.

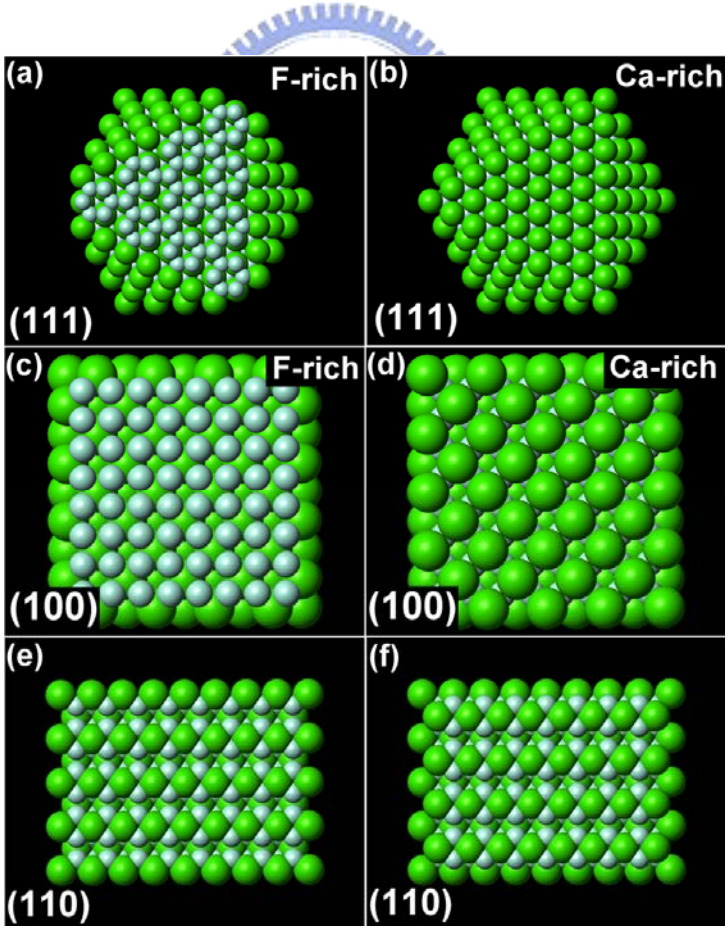

Figure 3.6 Surface models of CaF_2. {111} faces of (a) F-rich and (b) Ca-rich; {100} faces of (c) F-rich and (d) Ca-rich;(e) and (f) two types of {110} faces with equal Ca and F importance.

As mentioned above, in Figure 3.3, panels A and B, the CaF_2 core showed a preferred growth orientation in the [110] direction. Certain types of bonding and interaction between the core and the shell appear to be essential for this structural development (Figure 3.6). We suggest that at the *a*-C/CaF_2 interface, residual C-F bonds from the *a*-C shell layer could adhere to Ca exposed facets of CaF_2, such as {111} and {100}. This is analogous to the preferred interaction between small molecules such as water and methanoic acid on the CaF_2 surfaces.[19,20] In our case, the interaction would restrict the crystal growth in the [111] and [100] directions but enhance its elongation in the [110] direction (Figure 3.6). This phenomenon parallels the growth of CaF_2 nanostructures in {011} orientations on Si(001).[10] Here, the Si surface is bonded by the CaF_2 {111} facets.

We attempted to remove the carbon shell of **A** by reacting it with $O_{2(g)}$ at 773 K for 1h. SEM and EDS studies (Figure 3.7) indicated that the resulting material was pure CaF_2 nanowires with the carbon signal reduced to background noise. Thus we conclude that the process removed the carbon shell successfully. Also, the observation supports that the carbon concentration inside the CaF_2 core was very low indeed. We anticipate that the carbon shell can be removed from **B** by a similar process. The pure fluoride nanowires obtained this way may be employed as unique seeds for the growth of high quality optical crystals.

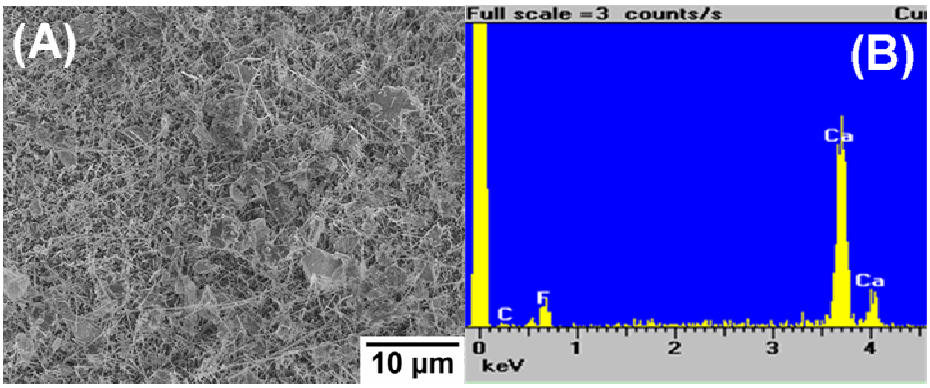

Figure 3.7 (A) A sample of CaF_2/*a*-C prepared at 973 K and reacted with O_2 at 773 K for 1 h to remove the *a*-C shell. (B) EDS of the nanowires shown in (A).

3.5 Conclusions

In conclusion, we have demonstrated the first time that 1-D CaF_2/*a*-C and MgF_2/*a*-C core/shell nanowires can be grown easily in one step via a simple VSRG process. The reaction proceeds without assistance from added template and catalyst materials, employment of special source of energies, and utilization of special pressure reactors.[13] Overall features of the process parallel other VSRG examples, such as growing cable-like Cu and Ag nanowires.[15,16] In VSRG, the reaction takes place at the vapor-solid interface, which is the surface of the solid reactant. Phase-separated solid products may develop into core/shell nanowires when the conditions are suitable. In this report, the successful growth of nanosized ionic-core/covalent-shell 1-D structures demonstrates the versatility of VSRG processes.

References

(1) Weast, R. C. *CRC Handbook of Chemistry and Physics,1st Student Edition* (CRC Press, Boca Raton, FL, **1988**).

(2) Harrison, W. A. *Electronic Structure and the Properties of Solids* (Dover, Mineola, NY, **1989**).

(3) *Kirk-Othmer Encyclopedia of Chemical Technology, Online Edition, http://www3.interscience.wiley.com/cgi-bin/mrwhome/104554789/HOME* (Wiley, New York).

(4) Burnett, J. H.; Levine, Z. H.; Shirley, E. L. *Phys. Rev. B* **2001,** *64*, 241102(R)-1.

(5) Watanabe, M.; Iketani, Y.; Asada, M. *Jpn. J. Appl. Phys. Pt. 2* **2000,** *39*, L964.

(6) Klust, A.; Kayser, R.; Wollschlager, J. *Phys. Rev. B* **2000,** *62*, 2158.

(7) Sata, N.; Eberman, K.; Eberl, K.; Maier, J. *Nature* **2000,** *408*, 946.

(8) Sayle, D. C.; Doig, J. A.; Parker, S. C.; Watson, G. W. *Chem. Comm.* **2003**, *15*, 804.

(9) Maria, W.; Michal, Z.; Mariusz, P. *J. Fluorine Chem.* **2003**, *120*, 1.

(10) Loretto, D.; Ross, F. M.; Lucas, C. A. *Appl. Phys. Lett.* **1996,** *68*, 2363.

(11) Viernow, J.; Petrovykh, D. Y.; Men, F. K.; Kirakosian, A.; Lin, J.-L.; Himpsel, F. J. *Appl. Phys. Lett.* **1999**, *74*, 2125.

(12) Sun, X.; Li, Y. *Chem. Commun.* **2003**, *14,* 1768.

(13) Xia, Y.; Yang, P.; Sun, Y.; Wu, Y.; Mayers, B.; Gates, B.; Yin, Y.; Kim, F.; Yan, H. *Adv. Mater.* **2003**, *15*, 353.

(14) Pan, Z. W.; Dai, Z. R.; Wang, Z. L. *Science* **2001,** *291*, 1947.

(15) Yen, M.-Y.; Chiu, C.-W.; Hsia, C.-H.; Chen, F.-R.; Kai, J.-J.; Lee, C.-Y.; Chiu, H.-T. *Adv. Mater.* **2003,** *15*, 235.

(16) Hsia, C.-H.; Yen, M.-Y.; Lin, C.-C.; Chiu, H.-T.; Lee, C.-Y. *J. Am. Chem. Soc.* **2003,** *125*, 9940.

(17) Johns, I. B.; Mcelhill, E. A.; Smith, J. O. *J. Chem. Eng. Data* **1962,** *7*, 277.

(18) *Reaction-Web, Facility for the Analysis of Chemical Thermodynamics*, *http://www.crct.polymtl.ca/fact/* (CRCT, École Polytechnique de Montréal: Montréal).

(19) de Leeuw, N. H.; Purton, J. A.; Parker, S. C.; Watson, G. W.; Kresse, G. *Surf. Sci.* **2000**, *452*, 9.

(20) de Leeuw, N. H.; Cooper, T. G. *J. Mater. Chem.* **2003,** *13*, 93.